

Adaptive coupling and enhanced synchronization in coupled phase oscillators

Quansheng Ren and Jianye Zhao

Department of Electronics, Peking University, Beijing 100871, China

(Received 17 December 2006; revised manuscript received 6 April 2007; published 10 July 2007)

We study the dynamics of an adaptive coupled array of phase oscillators. The adaptive law is designed in such a way that the coupling grows stronger for the pairs which have larger phase incoherence. The proposed scheme enhances the synchronization and achieves a more reasonable coupling dynamics for the network of oscillators with different intrinsic frequencies. The synchronization speed and the steady-state phase difference can be adjusted by the parameters of the adaptive law. Besides global coupling, nearest-neighbor ring coupling is also considered to demonstrate the generality of the method.

DOI: [10.1103/PhysRevE.76.016207](https://doi.org/10.1103/PhysRevE.76.016207)

PACS number(s): 05.45.Xt, 87.19.La

I. INTRODUCTION

Synchronization is a ubiquitous phenomenon in real world networks. As an important special case, the coordinated ensemble of coupled phase oscillators is a paradigm for many natural processes in physical, chemical, and biological systems [1], as well as in technological devices, such as Josephson junctions [2], laser arrays [3], neural networks [4], and phased antenna arrays [5,6]. These processes can be described with the Kuramoto model [7] and its extensions. The Kuramoto model describes the case of equal-strength all-to-all coupled phase oscillators, and its extensions have more general coupling, noise, external driving, etc. [8]. It was shown that, for certain purposes, networks with an appropriately tuned coupling matrix may be more reasonable. Seliger *et al.* [9] have proposed a state-dependent coupling scheme, whose learning principle is in such a way that the coupling strengthens for synchronized oscillators and weakens for nonsynchronized pairs. Their intention is to achieve information storage and retrieval. However, to achieve enhancement of global synchronization, different adaptive principles should be designed.

For Kuramoto-type phase oscillators, the ones near the center of the frequency distribution only need small coupling strength to lock together, while those in the tails need larger coupling strength to become synchronized. On the other hand, for a certain pair of oscillators, they need a large coupling strength to become rapid synchronized, but only need a sufficient coupling strength to maintain the synchronization. These observations lead to the following key question: How can we achieve a more reasonable coupling dynamics that synchronizes oscillators with different intrinsic frequencies?

Adaptive control is an important topic in control theory, and has attracted increasing interests in physical society recently [10]. The approach of adaptive control is that the system learns adaptively to find the best control law for the current estimate of the dynamical system. Sinha *et al.* [11,12] proposed the basic idea of using a dynamical property as feedback to adjust parameters to achieve the desirable value of the property. Several scholars [13–16] have applied the idea into the synchronization problem of chaotic oscillators. Nevertheless, the adaptation schemes already published are only in the simplest form. They could not be applied to phase oscillators such as Kuramoto's model to achieve an im-

proved dynamics. Another similar development in neuroscience is the characterization of spike-timing dependent plasticity (STDP) [17,18]. It was demonstrated that STDP greatly enhances the synchronization of neural ensembles with diverse membrane properties and intrinsic frequencies [19,20]. The self-adaptation dynamics leads the synaptic conductance to the value that is optimal for the entrainment of the postsynaptic. These results inspired us to design an adaptive principle to enhance the global synchronization of Kuramoto-type oscillators.

In this paper, we proposed a generalized Kuramoto model with adaptive coupling. The proposed adaptive scheme can enhance frequency synchronization of the whole network under general coupling architectures, and we study global coupling and nearest-neighbor ring coupling cases for instance. We mainly show that (i) the adaptive coupled Kuramoto model is closer to the real world cases and could achieve a more reasonable coupling dynamics. A measure of optimal coupling is introduced, and we show that our algorithm approaches to the optimal law according to it. (ii) The adaptation enhances the synchronization significantly compared to state-independent coupling where it is absent. (iii) The synchronization speed and steady-state phase difference can be adjusted by the parameters of the adaptive law, which could facilitate the applications in engineering and the understanding of certain natural phenomena. The paper is organized as follows. In Sec. II we introduce the generalized Kuramoto model and analyze the adaptive law theoretically. Global coupling and nearest-neighbor ring coupling cases are studied numerically in Sec. III. The dynamics of the adaptive coupling and the effect of the parameters are also examined in this section. Section IV summarizes our conclusions and gives some perspectives.

II. MODEL AND THE ADAPTIVE LAW

We consider the dynamics of an ensemble of N coupled phase oscillators,

$$\dot{\theta}_i = \omega_i - \frac{1}{N} \sum_{j=1}^N K_{ij} \sin(\theta_i - \theta_j). \quad (1)$$

Here ω_i are natural frequencies distributed with a given probability density $g(\omega)$, θ_i are phases of individual oscillators,

and K_{ij} is the $N \times N$ matrix of coupling coefficients. Throughout this paper, the number of units N is set to 50, as the results described below do not change qualitatively for larger systems. The initial values of the coupling coefficients were set to 0, and all the initial phase of the oscillators were randomly chosen from the interval $(0, 2\pi)$.

Heterogeneity in the intrinsic frequency distribution can suppress synchronization in networks of coupled phase oscillators with uniform coupling strength. This has been rarely considered to enhance the synchronization, and no practical method has been proposed in the literature. The most intuitive and ideal approach is to use a weighted network with asymmetric coupling $K_{ij} = C|\omega_i - \omega_j| \propto (\Delta\omega_{ij})^\mu$, which means that the coupling is proportional to the frequency difference $\Delta\omega_{ij} = |\omega_i - \omega_j|$ to an exponent $\mu = 1$. As the couplings are most positively correlated with the heterogeneity of the intrinsic frequencies, they will suppress the influence of heterogeneity furthest, and corresponds to the least average coupling cost. We consider the coupling scheme corresponding to $\mu = 1$ as optimum, and regard the exponent $\mu (\mu \leq 1)$ as the measure of optimum. The ‘‘optimum’’ here is in the sense of least average coupling cost for Kuramoto oscillators with different intrinsic frequencies. However, for lots of natural and practical systems, the intrinsic frequencies of oscillators could not be known in advance. Moreover, as the number of oscillators is huge, it is impossible to assign precalculated value to every coupling. Thus the forementioned approach ($K_{ij} = C|\omega_i - \omega_j|$) is unsuitable in practice.

The effective strategy is to use the adaptive method. We emphasize that the adaptive law used should approach the optimal coupling scheme, while it should also be realizable in practice. The Kuramoto model is not a toy model, but appears as a normal form for general systems of coupled oscillators. For facility of analysis, the standard simplification known as the phase approximation method [21,22] is used. However, in actual cases of weakly coupled oscillators, the phase parameter θ could not be obtained directly, but is represented in sine or cosine form. That is why we adopt the sinelike form in the paper, but not a linear adaptive function such as $\dot{K}_{ij} = \varepsilon[|\beta(\theta_i - \theta_j)| - K_{ij}]$ (suppose $\theta_{i,j} \in [-\pi, \pi]$). In this paper, the element of the coupling matrix describing interaction between two oscillators, for instance i and j , is controlled by the following equation

$$\dot{K}_{ij} = \varepsilon[\alpha|\sin(\beta(\theta_i - \theta_j))| - K_{ij}]. \quad (2)$$

In simulations, the parameters ε and β are fixed to 1 and 0.5, respectively. Later we will show how the behavior of the system changes as the function of the values of α , β , and ε . The comparison of performances between linear and sinelike adaptive functions will also be studied.

The adaptation function $\alpha|\sin(\beta(\theta_i - \theta_j))|$ implies that the coupling coefficient grows stronger for the pair of oscillators which has larger phase incoherence. This adaptation function is contrary to the form studied by Seliger [9], whose purpose is to obtain a multistable behavior. Figure 1 shows the learning curves of the adaptation function for different values of β . While the role of relative spike timing is played by the phase of oscillators, the curves are similar with the curve of

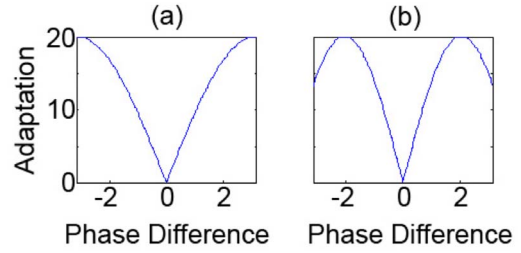


FIG. 1. (Color online) The learning curves of the adaptation function: (a) for $\alpha=20$ and $\beta=0.5$; (b) for $\alpha=20$ and $\beta=0.769$. In our study, we choose $\beta=0.5$ for maximum adaptive range of phase difference.

the additive STDP learning law [Fig. 3(a) in Ref. [20]] adopted by Nowotny *et al.* The learning curve of STPD could be symmetric about origin [19] or a shifted point in the x axis [20], while the learning curve we used is symmetric about the y axis. This difference could be ascribed to the directionality of coupling. For STPD, there is a presynaptic neuron and a postsynaptic neuron between a STDP synapse, and the time-dependent conductance of STDP synapses $g(t)$ is changed by $\Delta g(t)$, which is a function of the time difference $\Delta t = t_{post} - t_{pre}$. If a postsynaptic spike occurs sufficiently long after a presynaptic spike, the synaptic conductance is enhanced, while if a postsynaptic spike occurs close to or before a presynaptic spike, the synaptic conductance is depressed. This could be regarded as a directional coupling scheme. In our scheme, the coupling is a function of $\alpha|\sin(\beta(\theta_i - \theta_j))|$. The purpose is to drive the frequencies and phases together, and there are no distinctions such as pre- or postcoupling phase oscillators. It could be regarded as an unidirectional coupling scheme. Besides this, the essential ideas (learning and adaptive methods) of the STDP and our scheme are the same. Therefore, the adaptive law we proposed here has certain biological backgrounds, and is closer to the real world cases than ordinary Kuramoto models.

We expect the proposed scheme could approach to the optimal coupling scheme in the sense of least average coupling cost. To illustrate this point, we first consider a simple case of two oscillators. In this case, network system (1) and (2) reduces to

$$\dot{\phi} = \Delta\omega - K \sin \phi, \quad (3)$$

$$\dot{K} = \varepsilon(\alpha|\sin \beta\phi| - K). \quad (4)$$

Here $\phi = \theta_1 - \theta_2$, $K = K_{12} = K_{21}$, $\Delta\omega = \omega_1 - \omega_2$. Without loss of generality, suppose the coupling strength is large enough and a sufficiently small steady-state phase difference is achieved. Furthermore, assume the phase difference is positive and $0.5 \leq \beta \leq 1$, then $|\sin \beta\phi| \approx \beta \sin \phi$. When the two oscillators are synchronized and the coupling becomes steady, $\dot{\phi} = 0$, $\dot{K} = 0$, i.e.,

$$\Delta\omega - K \sin \phi = 0, \quad (5)$$

$$\varepsilon(\alpha\beta \sin \phi - K) = 0. \quad (6)$$

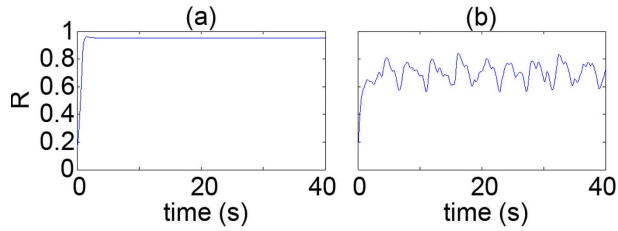


FIG. 2. (Color online) The evolution of the order parameter in the cases of (a) adaptive and (b) constant coupling for $\alpha=20$.

The solution is

$$\sin \phi = \sqrt{\Delta\omega/(\alpha\beta)},$$

$$K = \sqrt{(\alpha\beta)\Delta\omega} = C(\Delta\omega)^\mu,$$

where C (=const) determines the steady-state phase difference, and μ is the measure of optimum. For the case of two oscillators, $C = \sqrt{\alpha\beta}$ and $\mu=0.5$.

For the case of many coupled oscillators, we anticipate that the criterion μ will be increased, as the dynamics of an oscillator is influenced by more oscillators. Because the oscillator is influenced by the behavior of the whole network, it is difficult to obtain an analytical solution of the steady-state coupling strength K . However, from the numerical simulation described in Sec. III (Fig. 3) we find that the steady-state coupling strength is approximately $K_{ij} \propto (\Delta\omega_{ij})^\mu$. We have fitted the simulation results and found that $0.85 < \mu < 0.95$. Accordingly, the adaptive principle we proposed approaches to the optimal law, which corresponds to $\mu=1$.

III. PERFORMANCE ANALYSIS

The dynamics of a globally coupled array of oscillators is considered first. For universality, we consider the Gaussian distribution whose variance is 3 and a uniform distribution in the interval $(-3, 3)$. We studied the Gaussian distribution in two cases. (a) The adaptive coupling scheme. The steady-state coupling strength depends on the ratio of the frequency difference of two coupled oscillators. Its average value is equal to 3.385. (b) The constant coupling scheme whose strength is also 3.385. The complex order parameter $re^{i\psi} = (1/N)\sum_{j=1}^N e^{i\theta_j}$ is utilized to characterize the global behavior of the network. In Fig. 2(a) we see that the order parameter $r(t)$ achieves a constant value close to 1, which implies that the network of the adaptive coupling scheme have achieved global frequency synchronization and quasi phase coherence. In Fig. 2(b) we see that the order parameter $r(t)$ fluctuates between 0.6 and 0.8, which implies that the network of the constant coupling scheme with the same coupling cost could not achieve global frequency synchronization. In the constant coupling scheme, a fixed strength is used no matter what value the intrinsic frequency is. Thus the constant strength must be maximal to entrain the oscillator whose intrinsic frequency is highest, which means a kind of waste for others.

Then, we studied the network with a uniform frequency distribution in the interval $(-3, 3)$. As shown in Fig. 3(a), for

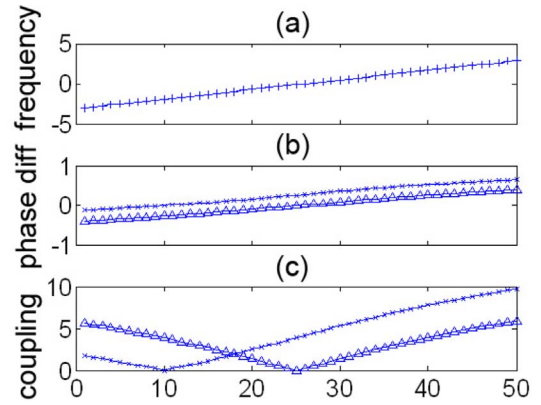


FIG. 3. (Color online) The relationship between (a) the intrinsic frequency distribution, (b) the steady-state phase difference, and (c) the steady-state coupling strength. Two cases are studied: the relations between the 10th and the other oscillators (X), and the relations between the 25th and the other oscillators (Δ).

the uniform frequency distribution, the i th oscillator's intrinsic frequency is $-3+0.12i$. Similar to the above, in Fig. 4(a) we see that the frequencies of all oscillators are equal, while a tiny constant phase drift is present between two frequency adjacent oscillators. However, oscillators in the constant coupling scheme with the same average coupling cost (3.477) have a confused phase evolution [Fig. 4(b)], i.e., the global synchronization could not be achieved.

Now we analyze the dynamics of the adaptive coupling in detail. According to the dynamic function $\dot{K}_{ij} = \varepsilon[\alpha|\sin(\beta(\theta_i - \theta_j))| - K_{ij}]$, we define the measure of phase difference between two coupled oscillators: $N = \alpha|\sin(\beta(\theta_i - \theta_j))|$. If two oscillators have different intrinsic frequencies, their phase difference is large in the beginning. Therefore $N \gg K_{ij}$ since the initial value of K_{ij} is zero. The coupling coefficient will increase continually, and the subsequent process should be analyzed in two cases: (a) If $N = K_{ij}$, but the two oscillators have not achieved synchronization, the increased coupling coefficient K_{ij} will drive the phase difference decrease. As a result, $N < K_{ij}$ and $\dot{K}_{ij} < 0$, which will lead to a decrease process of K_{ij} until the synchronization is achieved [Figs. 5(b) and 5(c)]. (b) If $N = K_{ij}$ and the two oscillators have achieved synchronization, the coupling dynamics will obtain a steady state [Fig. 5(d)]. Therefore, the adaptive dynamics shows

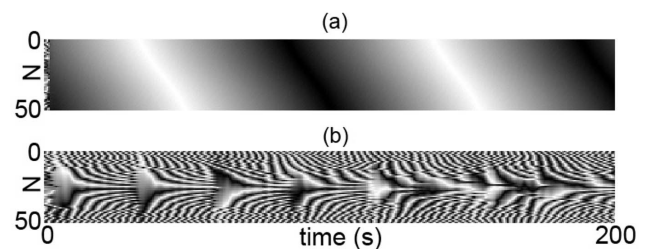


FIG. 4. Gray-scale plots of phase evolutions of 50 oscillators in the cases of (a) adaptive and (b) constant coupling for $\alpha=20$. The value of each gray-scale point is sampled every 0.5 s, and gray scale from white to black corresponds to the range $[-\pi, \pi]$.

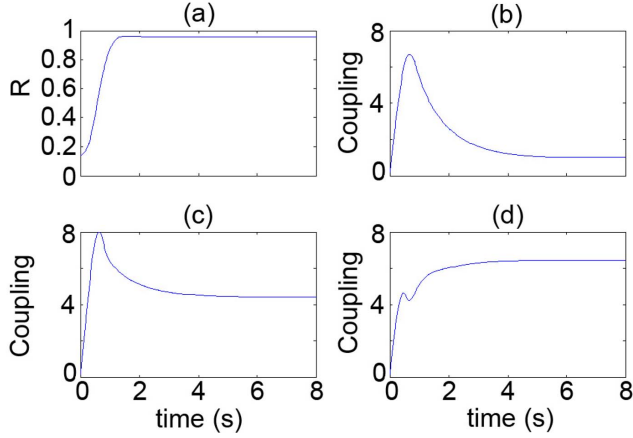


FIG. 5. (Color online) The evolutions of (a) the order parameter and the coupling coefficients: (b) $\kappa_{10,15}$, (c) $\kappa_{10,30}$, and (d) $\kappa_{10,40}$.

two possible behaviors, one in which it reaches the steady state from below and one in which it first overshoots the steady-state value and then reaches it from above. The last case implies that the coupling coefficient achieves a large strength to obtain rapid synchronization, while reduces to a sufficient strength to maintain the synchronization [Fig. 6]. When the coupling dynamics achieves a steady state, the coupling coefficient and the phase difference should satisfy the equation $N = \alpha |\sin(\beta(\theta_i - \theta_j))| = K_{ij}$, which is approximately a proportional relation, i.e., $K_{ij} \sim |\theta_i - \theta_j|$. On the other hand, two oscillators need a larger coupling strength if they have a larger intrinsic frequency difference [1]. The relationship between the steady-state coupling strength, phase difference, and frequency difference becomes more evident when we plot Fig. 3. The steady-state coupling strength is approximately $K_{ij} \propto (\Delta\omega_{ij})^\mu$, $0.85 < \mu < 0.95$, which approaches to the criterion of the optimal coupling law. From the above analysis, we see that an improved coupling dynamics is achieved.

Now we study the performance differences between different adaptive functions. We compare the proposed sinelike adaptive function with a linear adaptive function such as $\dot{K}_{ij} = \varepsilon [\alpha |\beta(\theta_i - \theta_j)| - K_{ij}]$ (suppose $\theta_{i,j} \in [-\pi, \pi]$). To compare them under the same conditions, we rewrite the linear adaptive function as $\dot{K}_{ij} = \varepsilon [\alpha |\arcsin[\sin(\beta(\theta_i - \theta_j))]| - K_{ij}]$, and the parameters ε and β are fixed to 1 and 0.5, respectively. We also examine how the system behavior of the sinelike adap-

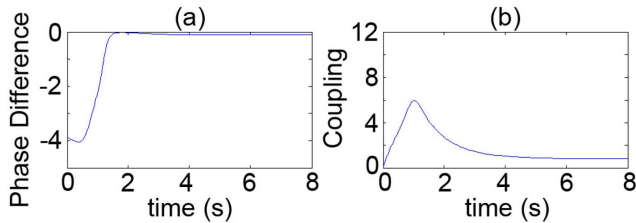


FIG. 6. (Color online) The evolution of (a) the phase difference versus the evolution of (b) the coupling coefficient between the 10th and the 15th oscillators in another simulation.

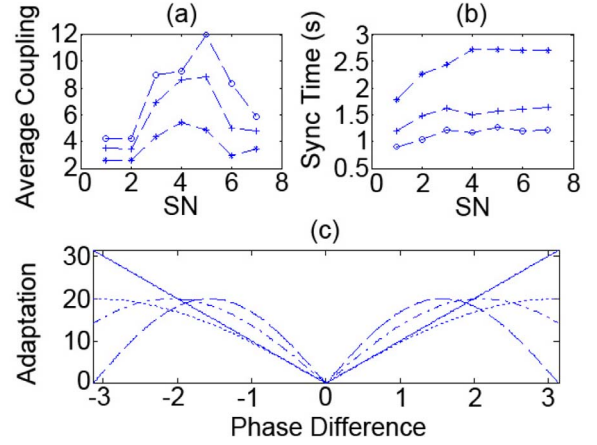


FIG. 7. (Color online) The comparison of performances between the linear adaptive scheme (serial number 1) and the sinelike adaptive schemes with different β are shown in (a) and (b). The serial numbers from 2 to 7 correspond to $\beta=0.5, 0.6, 0.7, 0.8, 0.9$, and 1.0 , respectively, and three cases are studied: $\alpha=10$ (*), $\alpha=20$ (+), and $\alpha=30$ (○). (c) The curves of different adaptive functions, including the linear adaptive function (—) and the sine-like adaptive functions with different β : $\beta=0.5$ (⋯), $\beta=0.75$ (---), and $\beta=1.0$ (--).

tive scheme changes with the values of β . The simulation results are illustrated in Fig. 7. We see that the average coupling costs of the linear and the sinelike adaptive schemes are the same, while the linear adaptive scheme has a little better performance in synchronization speed. For different settings of β , the sinelike adaptive scheme corresponding to $\beta=0.5$ has the best performances in the average coupling cost and synchronization speed. This could be ascribed to its monotonic increasing relation between the phase difference and the adaptation.

Then we examine the effect of the parameters ε and α . According to the dynamic equation $\dot{K}_{ij} = \varepsilon [\alpha |\sin(\beta(\theta_i - \theta_j))| - K_{ij}]$, for a larger parameter α , the coupling coefficient should increase further to achieve the steady state. As fore-mentioned, a larger coupling coefficient induces faster synchronization speed and smaller phase difference, and in turn induces the order parameter closer to 1. Therefore, the parameter α determines the magnitude of the steady-state coupling strength, phase difference, and the order parameter, which is illustrated in Fig. 8 and also determines the speed of synchronization. Rewriting the dynamic equation as

$$\frac{dK_{ij}}{d(\varepsilon t)} = \alpha |\sin(\beta(\theta_i - \theta_j))| - K_{ij},$$

we see that the parameter ε , as a time scale, only determines the evolution rate of the dynamic equation. Larger ε will accelerate the global synchronization. We have tested the relationship between the synchronization speed and the parameters (α, ε) in a large number of numerical simulations. The same random initial phase distribution was used for different (α, ε) in one simulation, and we simulated several times for different random initial phase distributions to obtain the average synchronization speed. To show the relationship more explicitly, we fitted the curve of simulation results further.

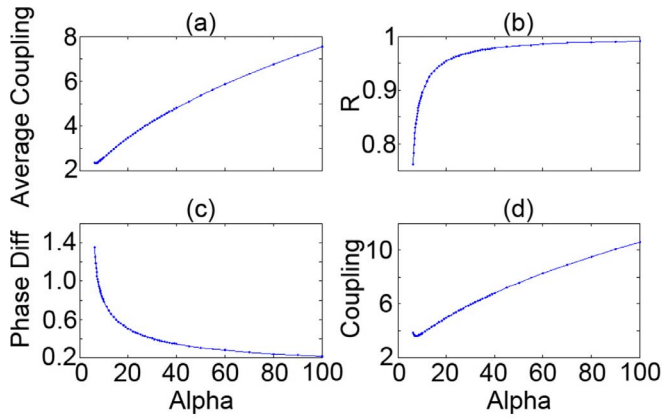


FIG. 8. (Color online) The parameter α (alpha) determines the steady-state magnitude of (a) the average coupling strength, (b) the order parameter, (c) the phase difference, and (d) the coupling strength. In (c) and (d), the relations between the 25th and the 50th oscillators are studied for instance.

The results are shown in Fig. 9. The fit functions for different α are

$$t_{syn} = \frac{1}{0.54 \ln(\varepsilon + 1) + 0.015} + 0.40, \quad \alpha = 10,$$

$$t_{syn} = \frac{1}{1.08 \ln(\varepsilon + 1) - 0.004} + 0.30, \quad \alpha = 20,$$

$$t_{syn} = \frac{1}{1.62 \ln(\varepsilon + 1) - 0.020} + 0.15, \quad \alpha = 30.$$

By ignoring the tiny correction terms, the functional dependence between the time taken for synchronization and the

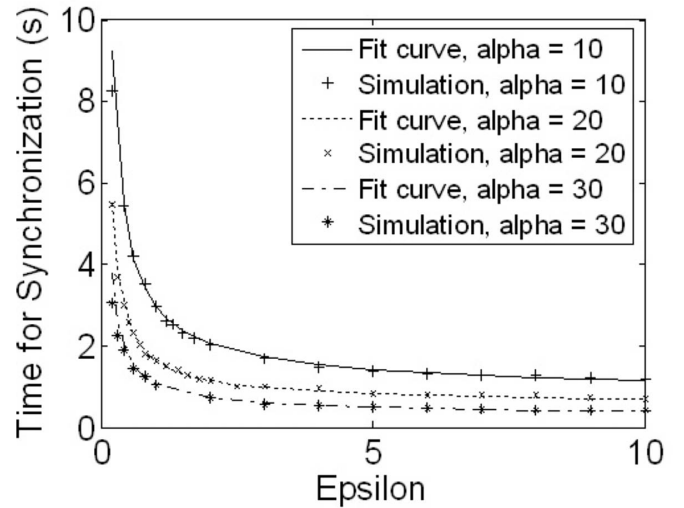


FIG. 9. The functional dependence between the time taken for synchronization and the parameters [α (alpha), ε (epsilon)]. Both simulation results (points) and fit curves (lines) are shown. The fit curves approximate to the function $t_{syn} = 1/[0.054\alpha \ln(\varepsilon + 1)]$.

parameters (α, ε) could be expressed by the following equation: $t_{syn} \approx 1/[0.054\alpha \ln(\varepsilon + 1)]$.

We stress that the adaptive coupling scheme proposed in this paper is general for the global synchronization problems of phase oscillators. To illustrate this generality, we also study the nearest-neighbor ring coupled phase oscillators. In the ring coupled configuration, the oscillators only interact with the right and left nearest-neighbor oscillators, so all oscillators are coupled similar to a ring. The dynamics of an ensemble of N coupled phase oscillators is

$$\dot{\theta}_i = \begin{cases} \omega_i - \frac{1}{2} \sum_{j=i-1}^{i+1} K_{ij} \sin(\theta_i - \theta_j), & \text{for } 1 < i < N, \\ \omega_i - \frac{1}{2} [K_{1N} \sin(\theta_1 - \theta_N) + K_{12} \sin(\theta_1 - \theta_2)], & \text{for } i = 1, \\ \omega_i - \frac{1}{2} [K_{N,N-1} \sin(\theta_N - \theta_{N-1}) + K_{N1} \sin(\theta_N - \theta_1)], & \text{for } i = N. \end{cases}$$

As the majority couplings are reduced, global synchronization is more difficult to achieve compared with the global coupling scheme. The case of Gaussian intrinsic frequency distribution is considered. For the adaptive coupling scheme, the result average value of the steady-state coupling strength is 8.689. As former cases, the constant coupling scheme with the same average value (8.689) cannot achieve global synchronization. Furthermore, when we use a larger constant coupling strength, 11, only partial synchronization could be achieved. This is showed in Fig. 10. We can see that all the

oscillators of the adaptive coupling scheme have invariable phase differences, while the oscillators of the constant coupling scheme is divided into at least two clusters.

IV. CONCLUSIONS AND PERSPECTIVES

In this paper we investigated the synchronization dynamics of the generalized Kuramoto model with adaptive coupling. With global adaptive coupling, the system dynamics approaches to the optimal coupling scheme in the sense of

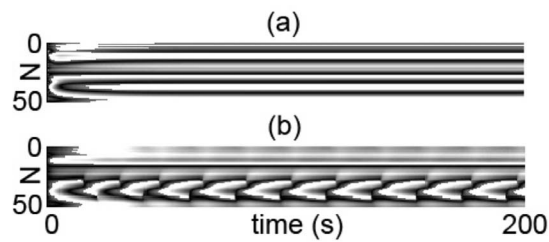


FIG. 10. Gray-scale plots of phase difference evolutions (versus the 17th oscillator) of 50 oscillators in the cases of (a) adaptive and (b) constant coupling for $\alpha=30$. The value of each gray-scale point is sampled every 0.5 s, and gray scale from white to black corresponds to the range $[-\pi, \pi]$.

least average coupling cost. The Gaussian and the uniform intrinsic frequency distributions are considered. In both cases, the ability of the networks to achieve synchronization is significantly enhanced, since the coupling intensities of oscillators are reduced adaptively according to their intrinsic frequencies. We also illustrate that the coupling coefficient achieves larger strength to obtain rapid synchronization in the transient process, while reduces to a smaller strength to maintain the synchronization in steady state. In this sense, an improved coupling dynamics is achieved.

The generalized Kuramoto model studied in this paper may serve as a paradigm for many biological and physical networks in which requirements of global synchronization

and coupling cost are strict. The best known examples of such networks are neuronal ensembles with adaptive coupling [19]. It is well known that in such a system, adaptive synaptic could enhance the synchronization significantly. Furthermore, for most biological systems, the intrinsic frequencies and other conditions of different parts are usually various, which implies that the coupling coefficients should be adapted to different circumstances. The proposed model will also shed light on some engineering applications, as the synchronization speed and phase coherence can be adjusted by the parameters of the adaptive equation.

In this paper we considered only two network architectures: a global coupled array and a nearest-neighbor coupled ring. Though we stress that the proposed scheme is a general method, the influence of the adaptive coupling on networks with more complex architecture is also an interesting open question. For example, in the case of complex network topologies, the adaptive coupling could be combined with the connectivity-dependent coupling [23], where the coupling strength depends on the number of links to or out of the node. Another interesting issue is the effect of adaptive coupling on the imperfect [24] and anomalous [25] phase synchronization of more complex chaotic oscillators. Because the increase of the coupling strength does not necessarily lead to better phase synchronization in these cases, the adaptive law should be improved further.

-
- [1] S. H. Strogatz, *Physica D* **143**, 1 (2000).
 [2] K. Wiesenfeld, P. Colet, and S. H. Strogatz, *Phys. Rev. E* **57**, 1563 (1998).
 [3] M. Silber, L. Fabiny, and K. Wiesenfeld, *J. Opt. Soc. Am. B* **10**, 1121 (1993).
 [4] F. C. Hoppensteadt and E. M. Izhikevich, *Weakly Connected Neural Networks* (Springer-Verlag, Berlin, 1997).
 [5] P. Liao and R. A. York, *IEEE Trans. Microwave Theory Tech.* **41**, 1810 (1993); T. Heath, K. Wiesenfeld, and R. A. York, *Int. J. Bifurcation Chaos Appl. Sci. Eng.* **10**, 2619 (2000).
 [6] M. Gabbay, M. L. Larsen, and L. S. Tsimring, *Phys. Rev. E* **70**, 066212 (2004).
 [7] Y. Kuramoto, *Chemical Oscillations, Waves, and Turbulence* (Springer, New York, 1991).
 [8] J. A. Acebrón *et al.*, *Rev. Mod. Phys.* **77**, 137 (2005).
 [9] P. Seliger, S. C. Young, and L. S. Tsimring, *Phys. Rev. E* **65**, 041906 (2002).
 [10] J. Bechhoefer, *Rev. Mod. Phys.* **77**, 783 (2005).
 [11] S. Sinha, R. Ramaswamy, and J. S. Rao, *Physica D* **43**, 118 (1990).
 [12] S. Sinha and N. Gupte, *Phys. Rev. E* **58**, R5221 (1998).
 [13] D. B. Huang, *Phys. Rev. Lett.* **93**, 214101 (2004).
 [14] D. B. Huang, *Phys. Rev. E* **71**, 037203 (2005).
 [15] Q. S. Ren and J. Y. Zhao, *Phys. Lett. A* **355**, 342 (2006).
 [16] C. Zhou and J. Kurths, *Phys. Rev. Lett.* **96**, 164102 (2006).
 [17] L. F. Abbott and S. B. Nelson, *Nat. Neurosci.* **3**, 1178 (2000).
 [18] M. I. Rabinovich *et al.*, *Rev. Mod. Phys.* **78**, 1213 (2005).
 [19] V. P. Zhigulin, M. I. Rabinovich, R. Huerta, and H. D. I. Abarbanel, *Phys. Rev. E* **67**, 021901 (2003).
 [20] T. Nowotny *et al.*, *J. Neurosci.* **23**(30), 9776 (2003).
 [21] M. Gabbay, M. L. Larsen, and L. S. Tsimring, *Proc. SPIE* **5559**, 146 (2004).
 [22] P. S. Hagan, *SIAM J. Appl. Math.* **42**, 762 (1982).
 [23] A. E. Motter, C. Zhou, and J. Kurths, *Europhys. Lett.* **69**, 334 (2005).
 [24] M. A. Zaks, E. H. Park, M. G. Rosenblum, and J. Kurths, *Phys. Rev. Lett.* **82**, 4228 (1999).
 [25] B. Blasius, E. Montbrió, and J. Kurths, *Phys. Rev. E* **67**, 035204(R) (2003).